Non-enzymatic methane formation by aerobic organisms

Leonard Ernst
Max-Planck-Institute for terrestrial Microbiology https://orcid.org/0000-0003-3994-8192
Benedikt Steinfeld
Max-Planck-Institute for Terrestrial Microbiology
Thomas Klintzsch
Heidelberg University
Dirk Grimm
University Hospital Heidelberg https://orcid.org/0000-0001-6227-5665
Ilka Bischofs
Universität Heidelberg
Frank Keppler (frank.keppler@geow.uni-heidelberg.de)
Heidelberg University https://orcid.org/0000-0003-2766-8812

Biological Sciences - Article

Keywords: Methane, Bacillus subtilis, CH4 cycling

Posted Date: March 1st, 2021

DOI: https://doi.org/10.21203/rs.3.rs-153741/v1

Version of Record: A version of this preprint was published at Nature on March 9th, 2022. See the published version at https://doi.org/10.1038/s41586-022-04511-9.

Abstract

Methane (CH4) is the most abundant organic compound in the atmosphere, largely originating from anthropogenic and natural biogenic sources1. Traditionally, biogenic CH4 has been regarded as the final product of the anoxic decomposition of organic matter by methanogenic Archaea. However, plants2–4, fungi5, algae6,7 and cyanobacteria8 have recently been shown to produce CH4 in the presence of oxygen. While methanogens produce CH4 enzymatically during anaerobic energy metabolism9, the requirements and pathways for CH4 production by “non-methanogenic” cells are poorly understood. Here we demonstrate that CH4 formation by Bacillus subtilis is triggered by free iron species, enhanced by oxidative stress and restricted to metabolically active life-cycle stages. We also show that other model organisms from Bacteria and Eukarya including a human cell line release CH4 and respond to inducers of oxidative stress by enhanced CH4 formation. Our results imply that all living cells possess a common mechanism of CH4 formation without the need for specific enzymes. We propose that CH4 formation is a conserved feature of living systems which is coupled to metabolic activity and the concomitant generation of reactive oxygen species. Our findings open new perspectives for our understanding of environmental CH4 cycling, oxidative stress responses and the search for extraterrestrial life.

Background

Methane is a highly potent greenhouse gas that affects Earth’s climate. Around 70 % of all emissions to the atmosphere derive from biogenic sources[10]. Biological CH_4 formation has long been considered to occur only under strictly anoxic conditions in organisms belonging to the domain *Archaea*. To generate the cellular fuel ATP, methanogenic archaea convert simple compounds, such as CO_2, H_2 or acetate, into CH_4. This process of methanogenesis depends on reactions that are catalysed by unique sets of enzymes and co-enzymes[9]. In addition, small amounts of CH_4 can be formed via ‘mini-methanogenesis’ in several sulphate-reducing bacteria which contain the enzyme carbon monoxide dehydrogenase[11,12]. However, during the past 15 years, evidence has been accumulating that other organisms produce CH_4 under aerobic conditions. These include both multicellular organisms, such as plants[2–4] and saprotrophic fungi[5], and unicellular organisms, including marine and freshwater algae[6,13] and cyanobacteria[8]. These organisms generate energy via photosynthesis and/or respiration, and it is unclear why and how they release CH_4. Multiple marine and freshwater bacteria harbouring the C-P lyase pathway have been reported to generate CH_4 from methylphosphonate[14–18]. Several bacteria and archaea have also been shown to possess alternative nitrogenases[19,20] or nitrogenase-like reductases[21], which can produce CH_4 and other hydrocarbons. In addition – as we will demonstrate here – living systems can form CH_4 without the need for specific enzymes, and such pathways could drive CH_4 formation in all cells.

In plants, CH_4 formation is enhanced by UV irradiation[3,22,23], inhibition of cytochrome *c* oxidase[24] and environmental stressors[4,25]. This raises the question whether reactive oxygen species (ROS, e.g., hydrogen peroxide H_2O_2, hydroxyl radicals ·OH and superoxide radicals O_2^-) might be involved in the

formation of CH_4. In highly oxidizing environments generated *in vitro* by a chemical model system containing iron (II/III), hydrogen peroxide (H_2O_2) and the radical scavenger ascorbic acid, CH_4 is readily formed from organosulphur compounds at ambient temperatures[26]. Under Fenton-type conditions, non-heme oxo-iron(IV) ($[Fe^{IV}=O]^{2+}$) oxidizes methyl sulphides to sulphoxides, which then results in selective formation of methyl radicals by sulphoxide demethylation, and ultimately leads to CH_4 and methanol formation depending on oxygen availability[26,27]. Moreover, ROS such as ·OH and H_2O_2 react with methyl sulphoxides to produce methyl radicals or peroxomethyl radicals in the presence of oxygen[28], subsequently resulting in generation of CH_4 or oxidized C_1 species.

Fenton chemistry takes place in living cells, as iron is an essential trace element[29] and H_2O_2 is produced during metabolism[30]. Hydrogen peroxide and Fe^{2+} react to either ferric iron (Fe^{3+}), OH^- and ·OH radicals, or alternatively $[Fe^{IV}=O]^{2+}$ and water[31]. This therefore raises the possibility that non-enzymatic CH_4 formation occurs in cells under oxic conditions at ambient temperatures. Suitable methyl donors for CH_4 formation could, in principle, be derived from a wide spectrum of molecules containing sulphur- and/or nitrogen-bonded methyl groups, which are endogenously produced during cellular metabolism and exogenously secreted during natural product formation. Such methylated sulphur compounds include methionine, dimethylsulphoniopropionate (DMSP), dimethyl sulphide (DMS) and dimethyl sulphoxide (DMSO), which are ubiquitous in the environment[32]. Thus, we tested the hypothesis that a non-enzymatic pathway of CH_4 formation exists in all cells, which is based on interactions between ROS, iron and methyl donors (Fig. 1A).

Formation of methane by *Bacillus subtilis*

We first explored CH_4 formation in the Gram-positive model bacterium *Bacillus subtilis* which, to the best of our knowledge, is not known to release CH_4. To detect authentic CH_4 formation, we performed stable carbon isotope labelling experiments, using sterile media as baseline controls, and measured CH_4 in the headspace of atmospherically sealed bacterial cultures (Fig. 1B). We first investigated whether CH_4 could be derived from glucose, an abundant carbon source that is readily taken up and metabolized by *B. subtilis*. Indeed, small but significant amounts of CH_4 were formed in bacterial cultures from [$^{13}C_6$]-glucose (0.21 nmol, $p < 0.001$). Moreover, the corresponding ^{13}C-isotope values ($\Delta\delta^{13}C$; difference between culture and sterile media) were highly enriched (79 ± 1 ‰). This indicates that glucose metabolism in *B. subtilis* results in at least one precursor compound that contributes to the formation of CH_4. We next investigated whether *B. subtilis* could utilize methyl sulphide and methyl sulphoxide as exogenous precursor carbon compounds for CH_4 formation. In fact, addition of either ^{13}C-labelled DMS or DMSO to bacterial cultures resulted in a clear shift in the isotopic value, demonstrating that the methyl groups of each sulphur compound were converted into CH_4 by reduction. Addition of DMSO increased CH_4 formation by 8-fold (1.85 nmol, $p < 0.001$) relative to glucose. Formation of CH_4 containing ^{13}C-labelled carbon derived from DMS was also observed. Although in the latter case CH_4 amounts were low,

and varied from experiment to experiment, $\Delta\delta^{13}C$ values were correlated with the amount of CH_4 produced. Taken together, these experiments provide unambiguous evidence for CH_4 formation from both exogenous and endogenous carbon compounds by *B. subtilis*.

Free iron and oxidative stress promote CH_4 formation

We further tested our hypothesis by varying the availability of suitable methyl donors, free iron and the level of oxidative stress, respectively (Fig. 1C). To minimize the effects of biomass variation on CH_4 formation, we used the same stationary-phase culture in a minimal medium and systematically varied the reaction conditions for CH_4 formation by supplying the substrate DMSO, additional free iron in the form of Fe^{2+} (as $FeSO_4$) and hypochlorous acid (HOCl) to induce oxidative stress in all possible combinations. The optical density (OD_{600nm}) of stationary cultures changes only marginally if at all (±1%), which implies that the observed variation in CH_4 can be attributed to increased CH_4 formation by *B. subtilis*. Under these conditions, external supply of DMSO (S) was required to stimulate significant CH_4 formation, as the amounts of CH_4 produced in its absence were close to atmospheric levels (Fig. 1C). In low-iron environments, addition of DMSO resulted in a small but significant quantity of CH_4 (0.45 nmol ± 0.03 nmol). Supplementation with HOCl to stimulate oxidative stress (S+O) increased this yield by ~40%. Moreover, an iron-rich environment (S+F) boosted CH_4 formation from DMSO by 17-fold, while the additional imposition of HOCl-induced oxidative stress (S+F+O) resulted in a 35-fold increase in CH_4 levels relative to substrate alone (S). In contrast, heat-inactivated *B. subtilis* released only marginal amounts of CH_4 (0.038 ± 0.006 nmol, $p = 0.007$) in conditioned media containing DMSO, Fe^{2+} and HOCl, suggesting that viable but not dead biomass promotes formation of CH_4. In accordance with our hypothesis, these data show that CH_4 formation from DMSO in stationary-phase *B. subtilis* cells is enhanced by both free iron and oxidative stress.

CH_4 formation is restricted to metabolically active life-cycle stages

According to our model, the generation of H_2O_2/ROS by living organisms is a prerequisite for CH_4 formation in the presence of suitable methyl donors. *B. subtilis* is a spore-forming organism that cycles between a dormant endospore state and a vegetative cell that grows and divides. Dormant spores are considered to be metabolically inactive, but resume metabolism upon germination[33]. DMSO readily enters dormant *Bacillus* spores and does not interfere with spore revival[34]. We thus asked whether the ability of *B. subtilis* to generate CH_4 from DMSO is restricted to its metabolically active life-cycle stages (Fig. 2A). To investigate this, we performed stable isotope labelling experiments on dormant and germinated *B. subtilis* spores using ^2H-labelled DMSO (Fig. 2B). The use of ^2H-labelled compounds and measurements of δ^2H values increases the detectability of CH_4 formation by orders of magnitude in comparison to ^{13}C labelling. Despite the exquisite sensitivity of the assay, CH_4 release from dormant spores after 10 h of incubation with DMSO was within the margin of error (0.02 nmol, $p = 0.066$), as were the stable hydrogen isotope signatures ($\Delta\delta^2H = 10 \pm 9$ ‰). In contrast, when spores were germinated by

supplying the nutrient germinant mixture AGFK, CH_4 formation was clearly detected (0.1 nmol, $P = 0.019$). Moreover, the stable hydrogen isotope signatures increased by three orders of magnitude, unambiguously confirming the conversion of the ^{2}H-labelled methyl group of ^{2}H-DMSO into CH_4 (Fig. 2B). Note that, under our experimental conditions, AGFK-induced germination is evidenced by the loss of spore refractivity; however, these spores did not grow out (Fig. 2B, insets). These data therefore suggest that germinated and thus metabolically active – but not dormant – spores can generate CH_4 from DMSO, in accordance with our hypothesis.

CH_4 accumulates during growth under oxic conditions

According to our model, CH_4 is mainly formed under oxic conditions. Since *B. subtilis* is a facultative anaerobe[35], we followed the dynamics of CH_4 accumulation during growth in complex media while monitoring the development of oxygen levels in the sample headspace (Fig. 2C). Methane levels increased during the exponential growth phase when oxygen was at atmospheric levels. Coincident with oxygen depletion, population growth slowed down rapidly, while CH_4 levels continued to increase for another ~ 2.5 h into stationary phase. Little additional CH_4 was formed during later cultivation stages when oxygen levels were low and the OD_{600nm} of the culture gradually declined. This indicates that *B. subtilis* forms CH_4 under oxic conditions, in agreement with our model.

Methane can be generated by organisms from all three domains of life

Finally, we investigated CH_4 formation by other cells from different domains of life that were previously not known to release CH_4. *Escherichia coli* DH5α served as a model organism for Gram-negative bacteria and *Corynebacterium glutamicum* ATCC 13032 for Gram-positive bacteria. The yeast *Saccharomyces cerevisiae* S288C and the mold *Aspergillus niger* DSM 821 served as fungal models. Human HEK293T cells were used as the model system for mammalian cells in particular and animals in general (Fig. 3A).

All microorganisms formed CH_4, and levels were enhanced under oxidative stress induced by the addition of HOCl (Fig. 3B). Cellular CH_4 formation by bacteria and fungi exceeded the respective (sterile) media controls by factors from ~1.1 minimum (non-stressed *S. cerevisiae*) to ~423 maximum (HOCl-stressed *A. niger*). We also observed CH_4 formation in HEK293T cells (Fig. 3C). Comparing culture and corresponding sterile media, CH_4 was formed by cultures supplemented with unlabelled DMSO (0.65 nmol, $P = 0.064$) or ^{2}H-DMSO (1.07 nmol, $P = 0.004$). Furthermore, the stable hydrogen isotope signatures of ^{2}H-labelled cultures clearly indicated that CH_4 is also formed from DMSO by mammalian HEK293T cells. Together with the well-established role of *Archaea* in producing CH_4, we conclude that organisms from all three domains of life release CH_4.

Discussion

In summary, our study strongly suggests that CH_4 is formed as a universal by-product of life, in addition to known CH_4 generation mechanisms by (mini-)methanogenesis[9,11], by alternative nitrogenases[19,20] and other enzymes[14,21] (e.g. C-P lyase). All organisms investigated here were not previously known to produce CH_4. Our results clearly demonstrate continuous formation of CH_4, which is substantially enhanced upon supplementation with free iron and induction of oxidative stress, in accordance with the proposed underlying mechanism. The use of position-specific $^{13}C/^{2}H$-labelled precursor compounds makes this clear. Under Fenton-type conditions, free iron species and H_2O_2 catalyse oxidative demethylation of methylated sulphur compounds. This in turn gives rise to methyl radicals and the subsequent formation of CH_4. Methane might also be released from other methylated components (bonded to nitrogen and oxygen) as previously indicated by a chemical model system[26]. In general, ROS and H_2O_2 have multiple sources[30], including respiratory activity, cellular stress and enzymatic reactions carried out by cytochrome oxidases and other heme monooxygenases[36], which are found in all three domains of life. We therefore propose that CH_4 release is a conserved feature of living systems that is coupled to metabolic activity and the corresponding generation of ROS. This opens new perspectives for (i) our understanding of environmental CH_4 cycling, (ii) oxidative stress responses and the potential physiological role(s) of CH_4, and (iii) the search for extraterrestrial life.

Formation of CH_4 as a consequence of fundamental biological processes implies that living biomass in all of Earth's environmental compartments continuously releases a background amount of CH_4. Although the CH_4 production by the investigated organisms is relatively small, if compared to methanogenic Archaea living in anaerobic environments, CH_4 release from aerobic organisms into the atmosphere might be of relevance to the biogeochemical cycles of CH_4. This has recently been proposed for cyanobacteria[8] and marine and freshwater algae[6,13] and their contribution to the abundance of CH_4 in oxygen-rich surface waters, commonly known as the "methane paradox"[18]. Note that it is not possible to quantitatively compare the amounts of CH_4 formed by the different organisms (e.g. on a dry weight basis) examined in our study. Determination of CH_4 production rates under field-like conditions requires an enormous experimental and analytical effort and must therefore await further studies.

Secondly, our results imply that the CH_4 formed in cells may be an integral part of their responses to changes in their oxidative status. Non-enzymatic formation of CH_4 was shown here to be coupled to cell metabolism. Moreover, in all investigated cells CH_4 release substantially increased under conditions that promote oxidative stress. Since many factors can cause secondary changes in oxidative stress in cells[37], these findings provide an explanation for elevated CH_4 formation under stress, which has previously been observed in plants[4,22,24,38], animals[39,40] and phototrophic organisms[4,8,41,42]. We therefore propose that CH_4 might serve as a read-out for stress and hypoxia[43]. For example, monitoring of variations in the CH_4 content in human breath has revealed age- and disease-dependent changes in cell metabolism[44,45]. Furthermore, it is conceivable that cells have evolved means to utilize CH_4 as a signalling molecule to

trigger adaptive stress responses[46,47]. This in turn could provide a rationale for the use of CH_4 as a therapeutic gas[43,48]. In this context, it has been shown that supplementation of CH_4 in animals has anti-inflammatory effects[49,50] and strengthens defences against organ dysfunction[51], and in plants the gas might enhance the antioxidant system[38].

Finally, the search for extraterrestrial life is in large part facilitated by analysing the atmospheric chemical signatures of exoplanets[52]. Enhanced atmospheric O_2 concentrations of rocky exoplanets are often regarded as a biosignature of photosynthesis[53]. As we now show that CH_4 is most probably formed under oxidative conditions by all non-methanogenic organisms in addition to anaerobe methanogenesis, we suggest that atmospheric CH_4 levels above the chemical equilibria might provide an additional and universal constraint of life on exoplanets, especially those with an O_2-rich atmosphere. Conversely, exoplanets with no traces of methane are proposed to be unlikely to host life.

Methods

Culture conditions

All CH_4 measurements were performed in sealed 60-mL glass vials containing 30 mL of culture medium. Cultures were incubated in a standard medium with the indicated supplements on a Multitron II at 37 °C and 180 rpm (unless otherwise specified) for the indicated times, and the concentration of CH_4 in the sample headspace was determined. All strains are listed in Supplementary Table 1.

B. subtilis cultivations

For ^{13}C labelling experiments, *Bacillus subtilis* 168 (1A700) was grown in S7-50 minimal medium[54] (starting OD_{600nm} = 0.01) and incubated for 12 h in the presence of 4% fully ^{13}C-labelled and 96 % unlabelled substrates: [$^{13}C_6$]-glucose (present at 1% in S7-50; Sigma Aldrich, Germany) or 10 mM [$^{13}C_2$]-DMSO or [$^{13}C_2$]-DMS (Campro Scientific GmbH, Germany), respectively. Sterile media and unlabelled cultures served as controls.

To modulate CH_4 formation, *B. subtilis* was first grown for 10 h to stationary phase in a shaken flask culture in S7-50 medium containing reduced levels of iron (50 nM $FeSO_4$). Cultures were then split and supplemented with substrate 200 mM DMSO (S), 4.95 µM $FeSO_4$ (Fe) and 300 µg mL^{-1} HOCl to induce oxidative stress (O). CH_4 was measured after 6 h. To inactivate biomass, cell suspensions were heated (90 °C for 30 min), washed with pure H_2O and resuspended in filtered, cell-free conditioned media containing chloramphenicol (5 µg mL^{-1}) and the indicated supplements.

For ^2H labelling experiments, *B. subtilis* spores ($5*10^7$ mL^{-1} derived from sporulation in liquid SM media[55]) were incubated in 25 mM TRIS-HCl buffer (pH = 7) containing 5 µM $FeSO_4$, 10 mM DMSO (unlabelled or labelled with 5% ^2H) for 10 h. Germination was induced by adding 3 mL of AGFK (19.8 mM

L-asparagine, 33.6 mM D-glucose, 33.6 mM D-fructose and 60 mM KCl). Germination was assessed by brightfield microscopy of spores on agarose pads[56] using a DeltaVision Elite Imaging System.

To measure CH_4 accumulation dynamics during growth, *B. subtilis* was grown in LB medium (starting OD_{600nm} = 0.01) without any supplements.

Cultivation of other organisms

Unless specified otherwise, cultures were inoculated to an OD_{600nm} = 0.01 from an overnight culture and shaken in a standard growth medium supplemented with 0.5 µM $FeSO_4$ and 10 mM DMSO. CH_4 was analysed after the indicated incubation time. Where applicable, oxidative stress was induced by the addition of 300 µg mL^{-1} HOCl. *Escherichia coli* DH5α was incubated in LB medium for 8 h. *Corynebacterium glutamicum* ATCC 13032 was grown in Brain Heart Infusion (BHI) for 8 h. *Saccharomyces cerevisiae* S288C was incubated in Yeast Extract-Peptone-Dextrose (YPD) medium at 30 °C for 24 h. *Aspergillus niger* DSM 821 (starting from 5*104 mL^{-1} of spores derived from PDA plates) was incubated in Potato-Dextrose-Broth (PDB) at 30 °C for 120 h. HEK293T cells (starting from $6*10^5$ cells mL^{-1}) were grown in Dulbecco's Modified Eagle's Medium (DMEM) supplemented with 10 % Fetal Calf Serum (FBS), 50 nM $FeSO_4$ and 50 mM DMSO (unlabelled or labelled with 5% ^2H) at 50 rpm for 48 h.

Quantification of CH_4 (GC-FID)

CH_4 was quantified by gas-chromatography flame-ionization detection (GC-FID). Aliquots (6 mL) of the sample headspace were retrieved using a gas-tight syringe (20 mL BD Luer-Lok™, Becton Dickinson, Madrid, Spain) with a needle (Large Hub RN, Hamilton, Bonaduz, Switzerland) and injected into a gas chromatograph [a high-grade steel tube (column length 2 m, inner diameter 3.175 mm) packed with Molecular Sieve 5A 60/80 mesh from Supelco] connected to a flame-ionization detector (Shimadzu GC-14B). Levels were quantified by comparison of the measured CH_4 peak area to that of a reference standard containing 2192 parts per billion by volume (measured three times). Unless indicated otherwise, CH_4 formation was calculated by subtracting the level of CH_4 of sterile medium from that of the inoculated culture.

δ ^{13}C stable isotope measurements (GC-C-IRMS)

$\delta^{13}C$ values of CH_4 were determined by gas chromatography-combustion-isotope ratio mass spectrometry (GC-C-IRMS). Aliquots of sampled headspace gas were transferred to an evacuated sample loop (40 mL) and a cryogenic pre-concentration unit in order to trap CH_4. CH_4 was trapped on HayeSep D, separated from interfering compounds by GC and transferred to a gas chromatography-combustion-isotope ratio mass spectrometer (GC-C-IRMS). The system consists of a cryogenic pre-concentration unit that is directly connected to a HP 6890N GC (He flow rate: 1.8 mL min^{-1}; Agilent Technologies, Santa Clara, USA) fitted with a GS-Carbonplot capillary column (30 m * 0.32 mm i.d., d_f 1.5 µm; Agilent

Technologies) and a PoraPlot capillary column (25 m * 0.25 mm (i.d.), d_f 8 µm; Varian, Lake Forest, USA). The GC flow was coupled via a press-fit connector to a combustion reactor comprised of an oxidation reactor (ceramic tube (Al_2O_3), length 320 mm, inner diameter 0.5 mm, with oxygen-activated Cu/Ni/Pt wires inside; reactor temperature 960°C) and a GC Combustion III Interface (ThermoQuest Finnigan) to decompose CH_4 into CO_2. $^{13}C/^{12}C$ ratios were determined with a Delta^{PLUS}XL mass spectrometer (ThermoQuest Finnigan, Bremen, Germany). High-purity CO_2 (carbon dioxide 4.5, Messer Griesheim, Frankfurt, Germany) was used as the working monitoring gas. $^{13}C/^{12}C$ ratios ($\delta^{13}C$ values) are expressed in the conventional δ notation in per mil versus VPDB, calculated as: **see formula 1 in the supplementary files.**

$\delta^{13}C$ values were corrected using three reference standards of high-purity CH_4 with $\delta^{13}C$ values of –54.5 ± 0.2 ‰ (Isometric Instruments, Victoria, Canada), –66.5 ± 0.2 ‰ (Isometric Instruments) and –42.3 ± 0.2 ‰ (in-house), calibrated against International Atomic Energy Agency and NIST reference substances. Finally, the isotope difference ($\Delta\delta^{13}C$) between the mean $\delta^{13}C$ values of sample and non-supplemented media was calculated as $\Delta\delta^{13}C = \delta^{13}C_{sample} - \delta^{13}C_{media}$.

δ^2H stable isotope measurements (GC-TC-IRMS)

δ^2H values of CH_4 were determined via gas chromatography-temperature conversion-isotope ratio mass spectrometry (GC-TC-IRMS). Here, the same analytical set-up was applied as for $\delta^{13}C$ stable isotope measurements (changed He flow rate: 0.6 mL min^{-1}) but instead of combustion to CO_2 and H_2O, CH_4 was thermolytically converted (at 1450 °C) to hydrogen and carbon. After IRMS measurements, the obtained δ^2H values were corrected by using two reference standards of high-purity CH_4 with δ^2H values of –149.9 ± 0.2 ‰ (T-iso2, Isometric Instruments) and –190.6 ± 0.2 ‰ (in-house). All $^2H/^1H$ ratios (δ^2H values) are expressed in the conventional δ notation in per mil versus VSMOW, calculated as:

See formula 2 in the supplementary files.

Finally, the isotope difference ($\Delta\delta^2H$) between the mean δ^2H values of sample and non-supplemented media was calculated as $\Delta\delta^2H = \delta^2H_{sample} - \delta^2H_{media}$.

Oxygen measurements (GC-BID)

The atmospheric oxygen content was determined via gas chromatography-barrier discharge ionization detection (GC-BID) using a GC-2010 Plus (Shimadzu, Japan). The GC-2010 (Shimadzu, Japan) comprises a stainless-steel ShinCarbon ST packed column (80/100 mesh; length: 2 m; diameter: 0.53 mm). The GC was operated with an injection temperature of 230 °C and an injection volume of 50 µL. Helium 6.0 (ALPHAGAZ, Air Liquide, France) served as the carrier gas with a flow rate of 50 mL min^{-1}. The temperature of the GC oven was held at 30 °C for 6.5 min, increased to 75 °C at a rate of 10 °C/min and then rising to 180 °C at a rate of 30 °C/min. The oxygen content of the sample was determined by

comparing the obtained O_2 peak with a sample of atmospheric air (O_2 content 20.95%). The calibration was conducted with five dilution steps.

Statistics

Unless otherwise indicated, all experiments were performed with N = 3 biological replicates. To test for significant differences in CH_4 formation between the samples, single-factor analysis of variance (ANOVA) was used.

Declarations

ACKNOWLEDGEMENTS

We thank M. Schneider, M. Schroll, M. Greule, B. Knape, C. Kaspar, Y. Gietz and L. Dietz for technical support, M. Baumgart, M. Knop and R. Fischer for providing strains, R. Thauer and J. Rebelein for critical comments and P. Hardy for editing the manuscript.

AUTHOR CONTRIBUTIONS

Designed research: LE, IB, FK. Performed experiments: LE, TK. Analyzed Data: LE, BS, TK, IB, FK. Supervised research: IB, DG, FK. Wrote the manuscript: LE, IB, FK.

AUTHOR INFORMATION

The authors declare no competing financial interests.

FUNDING

This work was supported by funds from the Max Planck Society (IB) and the Landesgraduiertenstiftung Baden-Württemberg (BS). FK, TK and DG were supported by the German Research Foundation (DFG; KE 884/8-2 and KE 884/16-2).

References

1. Saunois, M. *et al.* The global methane budget 2000-2017. *Earth Syst. Sci. Data***12,** 1561–1623 (2020).
2. Keppler, F., Hamilton, J. T. G., Braß, M. & Röckmann, T. Methane emissions from terrestrial plants under aerobic conditions. *Nature***439,** 187–191 (2006).
3. McLeod, A. R. *et al.* Ultraviolet radiation drives methane emissions from terrestrial plant pectins. *New Phytol.***180,** 124–132 (2008).
4. Martel, A. B., Taylor, A. E. & Qaderi, M. M. Individual and interactive effects of temperature and light intensity on canola growth, physiological characteristics and methane emissions. *Plant Physiol. Biochem.***157,** 160–168 (2020).

5. Lenhart, K. *et al.* Evidence for methane production by saprotrophic fungi. *Nat. Commun.***3,** 1–8 (2012).
6. Klintzsch, T. *et al.* Methane production by three widespread marine phytoplankton species: Release rates, precursor compounds, and potential relevance for the environment. *Biogeosciences***16,** 4129–4144 (2019).
7. Lenhart, K. *et al.* Evidence for methane production by the marine algae Emiliania huxleyi. *Biogeosciences***13,** 3163–3174 (2016).
8. Bižić, M. *et al.* Aquatic and terrestrial cyanobacteria produce methane. *Sci. Adv.***6** doi:10.1126/sciadv.aax5343 (2020).
9. Thauer, R. K. Biochemistry of methanogenesis: a tribute to Marjory Stephenson:1998 Marjory Stephenson Prize Lecture. *Microbiology***144,** 2377–2406 (1998).
10. Conrad, R. The global methane cycle: Recent advances in understanding the microbial processes involved. *Environ. Microbiol. Rep***1,** 285–292 (2009).
11. Schauder, R., Eikmanns, B., Thauer, R. K., Widdel, F. & Fuchs, G. Acetate oxidation to CO2 in anaerobic bacteria via a novel pathway not involving reactions of the citric acid cycle. *Arch. Microbiol.***145,** 162–172 (1986).
12. Vorholt, J., Kunow, J., Stetter, K. O. & Thauer, R. K. Enzymes and coenzymes of the carbon monoxide dehydrogenase pathway for autotrophic CO2 fixation in Archaeoglobus lithotrophicus and the lack of carbon monoxide dehydrogenase in the heterotrophic A. profundus. *Arch. Microbiol.***163,** 112–118 (1995).
13. Hartmann, J. F. *et al.* High Spatiotemporal Dynamics of Methane Production and Emission in Oxic Surface Water. *Environ. Sci. Technol.***54,** 1451–1463 (2020).
14. Kamat, S. S., Williams, H. J., Dangott, L. J., Chakrabarti, M. & Raushel, F. M. The catalytic mechanism for aerobic formation of methane by bacteria. *Nature***497,** 132–136 (2013).
15. Gomez-Garcia, M. R., Davison, M., Blain-Hartnung, M., Grossman, A. R. & Bhaya, D. Alternative pathways for phosphonate metabolism in thermophilic cyanobacteria from microbial mats. *ISME J.***5,** 141–149 (2011).
16. Yao, M., Henny, C. & Maresca, J. A. Freshwater bacteria release methane as a by-product of phosphorus acquisition. *Appl. Environ. Microbiol.***82,** 6994–7003 (2016).
17. Beversdorf, L. J., White, A. E., Björkman, K. M., Letelier, R. M. & Karl, D. M. Phosphonate metabolism of Trichodesmium IMS101 and the production of greenhouse gases. *Limnol. Oceanogr.***55,** 1768–1778 (2010).
18. Metcalf, W. W. *et al.* Synthesis of methylphosphonic acid by marine microbes: a source for methane in the aerobic ocean. *Science***337,** 1104–1107 (2012).
19. Rebelein, J. G., Lee, C. C., Hu, Y. & Ribbe, M. W. The *in vivo* hydrocarbon formation by vanadium nitrogenase follows a secondary metabolic pathway. *Nat. Commun.***7,** 1–6 (2016).

20. Zheng, Y. *et al.* A pathway for biological methane production using bacterial iron-only nitrogenase. *Nat. Microbiol.***3,** 281–286 (2018).
21. North, J. A. *et al.* A nitrogenase-like enzyme system catalyzes methionine, ethylene, and methane biogenesis. *Science* **369,** 1094–1098 (2020).
22. Vigano, I. *et al.* Effect of UV radiation and temperature on the emission of methane from plant biomass and structural components. *Biogeosciences***5,** 937–947 (2008).
23. Keppler, F. *et al.* Methoxyl groups of plant pectin as a precursor of atmospheric methane: Evidence from deuterium labelling studies. *New Phytol.***178,** 808–814 (2008).
24. Wishkerman, A. *et al.* Enhanced formation of methane in plant cell cultures by inhibition of cytochrome c oxidase. *Plant Cell Environ***34,** 457–464 (2011).
25. Abdulmajeed, A. M. & Qaderi, M. M. Differential effects of environmental stressors on physiological processes and methane emissions in pea (Pisum sativum) plants at various growth stages. *Plant Physiol. Biochem.***139,** 715–723 (2019).
26. Althoff, F. *et al.* Abiotic methanogenesis from organosulphur compounds under ambient conditions. *Nat. Commun.***5,** 1-9 (2014).
27. Benzing, K., Comba, P., Martin, B., Pokrandt, B. & Keppler, F. Nonheme iron-oxo-catalyzed methane formation from methyl thioethers: scope, mechanism, and relevance for natural systems. *Chem. Eur. J.***23,** 10465–10472 (2017).
28. Herscu-Kluska, R., Masarwa, A., Saphier, M., Cohen, H. & Meyerstein, D. Mechanism of the reaction of radicals with peroxides and dimethyl sulfoxide in aqueous solution. *Chem. Eur. J.***14,** 5880–5889 (2008).
29. Kaplan, J. & Ward, D. M. The essential nature of iron usage and regulation. *Curr. Biol.***23,** 642–646 (2013).
30. Mittler, R. ROS are good. *Trends Plant Sci.***22,** 11–19 (2017).
31. Enami, S., Sakamoto, Y. & Colussi, A. J. Fenton chemistry at aqueous interfaces. *Proc. Natl. Acad. Sci. USA.***111,** 623–628 (2014).
32. Dunbar, K. L., Scharf, D. H., Litomska, A. & Hertweck, C. Enzymatic carbon-sulfur bond formation in natural product biosynthesis. *Chem. Rev.* **117,** 5521–5577 (2017).
33. Setlow, P. Germination of spores of *Bacillus* species: what we know and do not know. *J. Bacteriol.***196,** 1297–1305 (2014).
34. Ewing, D. The effects of dimethylsulfoxide (DMSO) on the radiation sensitivity of bacterial spores. *J. Radiat. Res.***90**, 348–355 (1982).
35. Nakano, M. M. & Zuber, P. Anaerobic growth of a 'strict aerobe' (*Bacillus subtilis*). *Annu. Rev. Microbiol.* **52,** 165–190 (1998).
36. Veith, A. & Moorthy, B. Role of cytochrome P450s in the generation and metabolism of reactive oxygen species. *Curr. Opin. Toxicol.***7,** 44–51 (2018).

37. Mols, M. & Abee, T. Primary and secondary oxidative stress in *Bacillus*. *Environ. Microbiol.***13,** 1387–1394 (2011).
38. Wang, N. *et al.* Regulatory roles of methane in plants. *Sci. Hortic.* **272** doi:10.1016/j.scienta.2020.109492 (2020).
39. Ghyczy, M. *et al.* Hypoxia-induced generation of methane in mitochondria and eukaryotic cells - an alternative approach to methanogenesis. *Cell. Physiol. Biochem.***21,** 251–258 (2008).
40. Tuboly, E. *et al.* Methane biogenesis during sodium azide-induced chemical hypoxia in rats. *Am. J. Physiol., Cell Physiol.* **304,** 207–214 (2013).
41. Klintzsch, T. *et al.* Effects of temperature and light on methane production of widespread marine phytoplankton. *J. Geophys. Res. Biogeosci.***125** doi:10.1029/2020JG005793 (2020).
42. Martel, A. B. & Qaderi, M. M. Unravelling the effects of blue light on aerobic methane emissions from canola. *J. Plant Physiol.***233,** 12–19 (2019).
43. Boros, M. & Keppler, F. Methane production and bioactivity - a link to oxido-reductive stress. *Front. Physiol.* **10,** doi:10.3389/fphys.2019.01244 (2019).
44. Polag, D., Leiß, O. & Keppler, F. Age dependent breath methane in the German population. *Sci. Total Environ.***481,** 582–587 (2014).
45. De Lacy Costello, B. P. J., Ledochowski, M. & Ratcliffe, N. M. The importance of methane breath testing: a review. *J Breath Res***7,** doi:10.1088/1752-7155/7/2/024001 (2013).
46. Zhang, B., Gao, M., Shen, J. & He, D. Inhaled methane protects rats against neurological dysfunction induced by cerebral ischemia and reperfusion injury: PI3K/Akt/HO-1 pathway involved. *Arch. Med. Res.***48,** 520–525 (2017).
47. Zhang, X. *et al.* Methane limit LPS-induced NF-κ B/MAPKs signal in macrophages and suppress immune response in mice by enhancing PI3K/AKT/GSK-3β-mediated IL-10 expression. *Sci. Rep.***6**, 1–14 (2016).
48. Ye, Z. heng, Ning, K., Ander, B. P. & Sun, X. jun. Therapeutic effect of methane and its mechanism in disease treatment. *J Zhejiang Univ Sci B***21,** 593–602 (2020).
49. Bari, G. *et al.* Methane inhalation reduces the systemic inflammatory response in a large animal model of extracorporeal circulation. *Eur J Cardiothorac Surg***56,** 135–142 (2019).
50. Jia, Y., Li, Z., Liu, C. & Zhang, J. Methane medicine: a rising star gas with powerful anti-inflammation, antioxidant, and antiapoptosis properties. *Oxid. Med. Cell. Longev.***2018,** 1–10 (2018).
51. Benke, K. *et al.* Methane-enriched custodiol preservation solution improves graft function in experimental model of heterotopic heart transplantation. *J. Heart Lung Transplant.***39,** 351–352 (2020).
52. Fox, S. & Strasdeit, H. Inhabited or uninhabited? Pitfalls in the interpretation of possible chemical signatures of extraterrestrial life. *Front. Microbiol.* **8,** 348–355 (2017).
53. Léger, A. *et al.* Is the presence of oxygen on an exoplanet a reliable biosignature? *Astrobiology***11,** 335–341 (2011).

54. Vasantha, N. & Freese, E. Enzyme changes during Bacillus subtilis sporulation caused by deprivation of guanine nucleotides. *J. Bacteriol.***144,** 1119–1125 (1980).

55. Harwood, C. R. & Cutting, S. M. *Molecular Biological Methods for* Bacillus. John Wiley & Sons Ltd, Chichester **1** (1990).

56. Mutlu, A. *et al.* Phenotypic memory in *Bacillus subtilis* links dormancy entry and exit by a spore quantity-quality tradeoff. *Nat. Commun.***9,** 1-12 (2018).

Figures

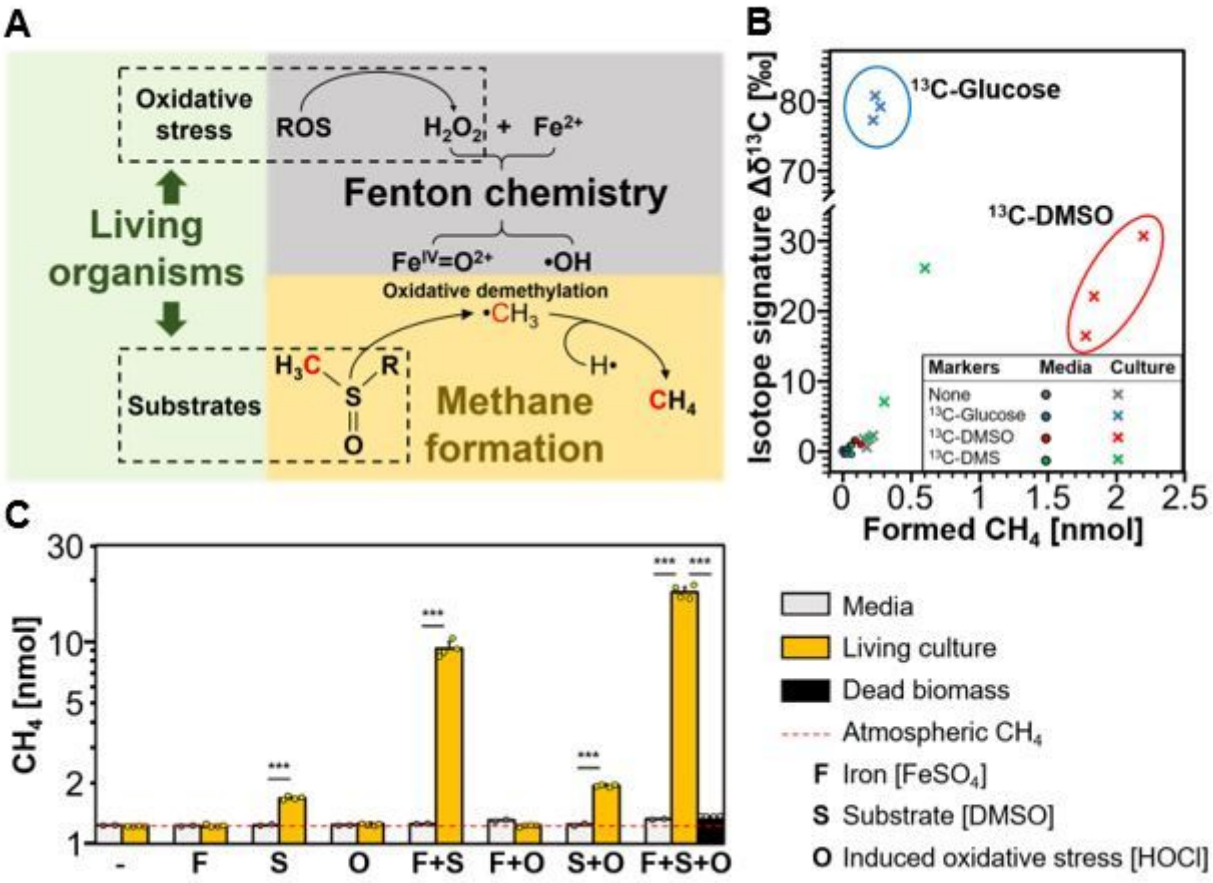

Figure 1

CH4 formation by B. subtilis. (A) Proposed mechanism of non-enzymatic CH4 formation in living systems. Organisms produce methyl donors such as organosulphur compounds and continuously generate H2O2 under oxidative stress, supplying substrates and favorable reaction conditions for CH4 formation. (B) B. subtilis forms CH4 from glucose and methyl groups of organosulphur compounds. Isotope signatures (Δδ13C between culture sample and control) and amounts of CH4 produced in the presence of the indicated substrates provide unambiguous evidence for CH4 formation from both glucose (blue) and DMSO (red). Data points represent individual measurements. (C) CH4 formation from DMSO (S) is significantly enhanced by Fe2+ (F) and HOCl (O). CH4 is formed in living cultures (orange),

but not in sterile media (grey) or in the presence of dead biomass (black). The dashed red line depicts the background (laboratory) CH4 content. Bars represent means ± SD, N = 4 biological replicates and N = 2 media replicates. ***: P ≤ 0.001.

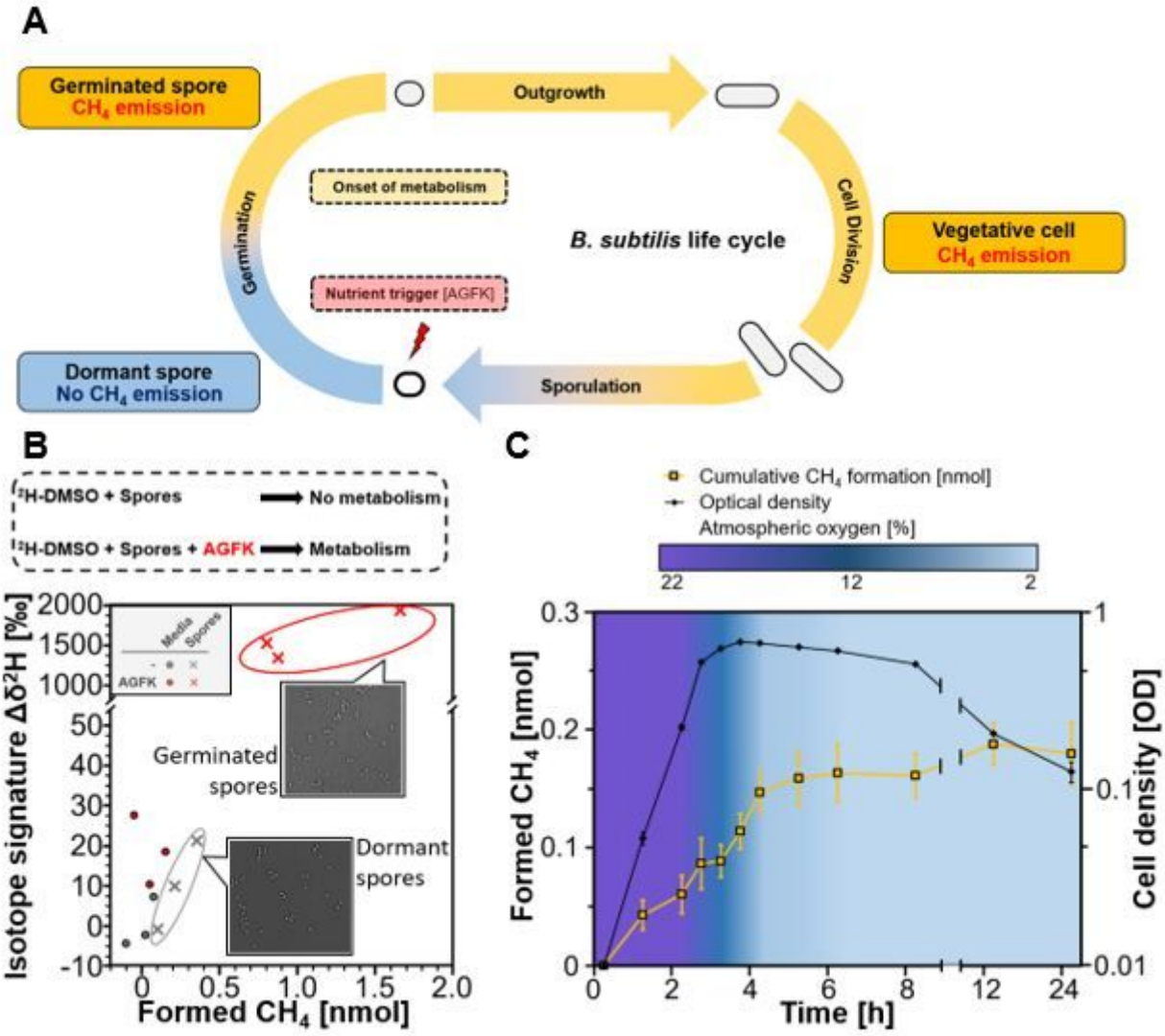

Figure 2

B. subtilis forms CH4 throughout its metabolically active life-cycle stages. (A) Life cycle of spore-forming B. subtilis bacteria depicting CH4 formation during metabolically active stages. (B) Germinated, but not dormant, B. subtilis spores generate CH4 from 2H-DMSO. Scatterplot depicting stable hydrogen isotope signatures (Δδ2H) and amounts of CH4 formed. Insets show bright-field micrographs of refractive dormant spores and non-refractive germinated spores. Data points represent individual measurements from N = 3 biological or media replicates. (C) CH4 accumulates during B. subtilis growth. The majority of CH4 formation occurs during exponential growth under oxic conditions, while little additional CH4 is formed during the stationary phase induced by oxygen depletion (blue color gradient). Cumulative CH4 levels (orange) and population growth (black) plotted as a function of time. Symbols represent means ± SD. from N = 2 biological replicates.

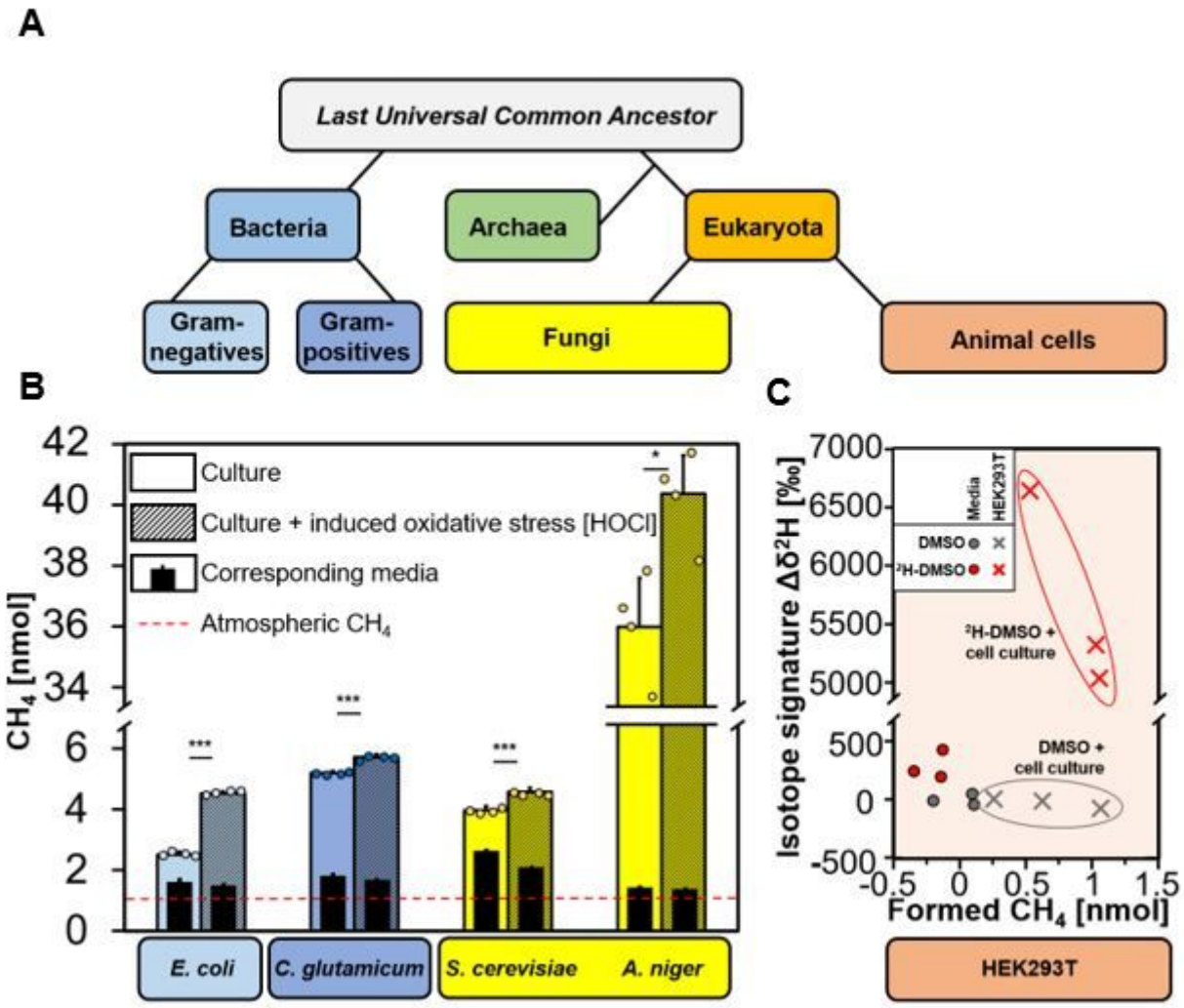

Figure 3

All lifeforms generate CH4. (A) Simplified tree of life. Non-enzymatic CH4 formation is proposed to occur in all living organisms, while methanogenic archaea also produce CH4 enzymatically. (B) Selected bacterial and fungal cells form CH4 under standard growth conditions (left bars) and under HOCl-induced oxidative stress (right bars). From left to right: Gram-negative Escherichia coli DH5α (cyan), Gram-positive C. glutamicum ATCC 13032 (dark blue), the yeast S. cerevisiae S288C and the mold A. niger DSM 821 (both yellow). Bars represent means ± SD from N = 4 biological replicates. Circles represent individual measurements. *: $P \leq 0.05$, ***: $P \leq 0.001$. (C) A human cell line converts deuterium-labelled 2H-DMSO into CH4. Scatterplot of stable hydrogen isotope signatures and CH4 amounts generated by HEK293T cells in the presence of isotopically labelled DMSO (red) and unlabelled DMSO (grey). Data points represent individual measurements from N = 3 biological or media replicates.

Supplementary Files

This is a list of supplementary files associated with this preprint. Click to download.

- formulas.docx